# Chapter 2

# Experimental method

## 2.1 Reaction mechanism

Compound nuclear reactions can populate continuum states of nuclear many-body systems. These states have high excitation energies, and therefore such reactions tend to involve complicated excitations involving many degrees of freedom. Reactions with these characteristics proceed further by the *compound-nucleus* (CN) mechanism. However, it may sometimes happen that only a few degrees of freedom are excited and that the other degrees of freedom of the many-body system effectively remain passive. Reactions that possess this simplicity are said to proceed by the *direct-reaction* (DR) mechanism. Cross-sections from both mechanisms are found experimentally and it is necessary to build theories that are adapted to both the CN and DR types. Often the reaction mechanism is analysed using two quite different theoretical techniques, with the DR analysis stressing detailed solutions of the Schrödinger equation and the CN analysis concentrating on statistical properties of the nuclear system. However, it is clear that both CN and DR types can be present simultaneously and that the two aspects of any given nuclear reaction must be considered. This is particularly true for reactions between light nuclei. A short description of both reaction mechanisms is given below.

### 2.1.1 Compound nuclear reactions

The idea of compound nucleus formation was first suggested by Niels Bohr in 1936 [Boh36]. In such a reaction $A_1 + A_2 \rightarrow C^*$, the target and the projectile fuse together, forming a *compound nucleus*, $C^*$. In this model several criteria must be satisfied:

• the projectile must have an energy large enough to overcome the Coulomb barrier ($E_{CB}$):

$$E_{CB}[MeV] = \frac{1.44 Z_1 Z_2}{1.16(A_1^{1/3} + A_2^{1/3} + 2)} \tag{2.1}$$

where $Z_1$ and $A_1$ are the atomic number and mass of the projectile respectively and $Z_2$ and $A_2$ are the corresponding values for the target nucleus.

• the angular momentum transfer should be small so that the centrifugal repulsion caused by the rotation of the nucleus does not overcome the short-range attraction of the nuclear force.

• all degrees of freedom of the compound system must be equally populated. The subsequent decay is governed by the phase space of the individual channels X; $A_1+A_2 \rightarrow C^* \rightarrow X+x$.

When formed, the compound nucleus will be in a state of high excitation energy. This excitation energy can be lost from the compound nucleus in several ways, as shown in Fig. 2.1. At high angular momenta the most probable way is *fission*. This is due to the fact that the nucleus is no longer stable against the centrifugal force caused by the rotation, which means that the attraction of the nuclear force can be overcome. If the compound nucleus does not undergo fission, the main part of the excitation energy is removed by *particle emission* (neutrons, protons and $\alpha$-particles). The evaporation of charged particles (protons and $\alpha$-particles) is normally suppressed by the Coulomb barrier. The evaporation of particles carries away a large amount of excitation energy (10-20 MeV) [Mor83], but a small amount of angular momentum. Thus, the evaporation of particles leaves the compound nucleus in a state of high angular momentum, and gives a

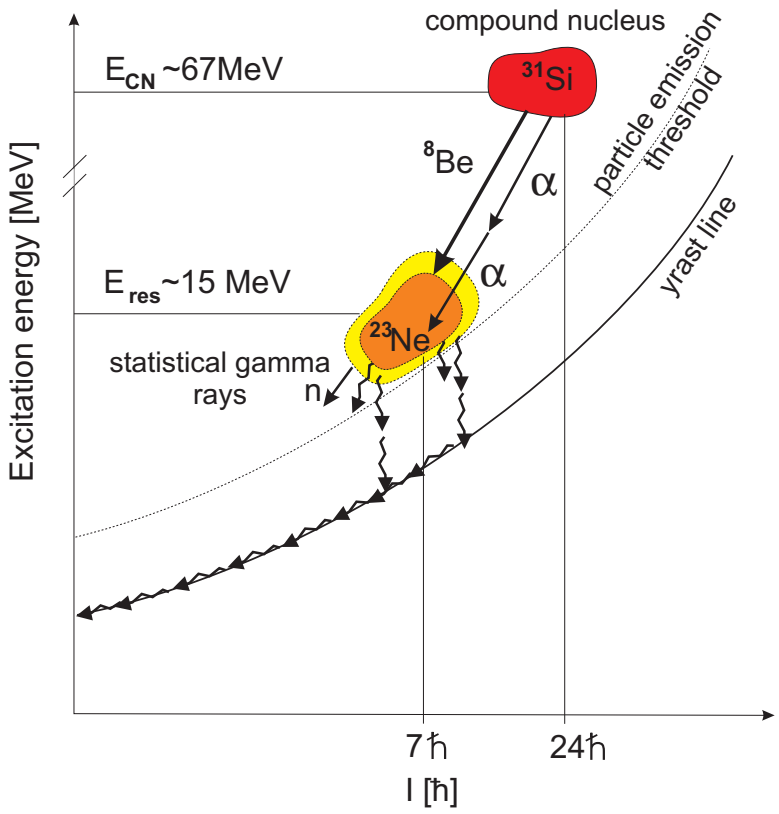


Figure 2.1: Diagram of the excitation energy of the compound nucleus, versus spin $I$. The scheme shows the decay of the compound nucleus via particle and $\gamma$-ray emission.

steep descent towards the ground state.

When the excitation energy is below the particle threshold the nucleus continues to de-excite via the emission of *statistical* $\gamma$-rays due to the very high density of states. These are usually dipole transitions (E1), carrying away energy, but again very little angular momentum. These $\gamma$-rays are normally not resolved in a $\gamma$-ray spectroscopy experiment. After the nucleus is cooled it reaches the *yrast* (which means *weary* in Swedish) region. The yrast line defines the states with the largest spin value, $I$, for a given excitation energy. The $\gamma$-ray emission continues via discrete $\gamma$-ray transitions (*e.g.* E2 decays), carrying away more angular momentum until the ground state is reached. These *yrast-like* transitions are

the most important from a spectroscopic point of view since they carry enough intensity to be isolated in a $\gamma$-ray spectrum and from them information about the studied nuclei can be extracted.

### 2.1.2 Direct reactions

In contrast to the compound nucleus reaction mechanism direct reactions involve direct passage from the initial to the final state, without the formation of any intermediate state.

#### Stripping reactions

The theory of stripping reactions was first outlined, for low energies and without discussion of angular momentum, by Oppenheimer and Philips [Opp35]. More detailed treatments, concerned especially with nuclear states using angular distributions to assign values of angular momentum to the states formed in stripping reaction at higher energies, have been published by Butler [But51] and by Bhatia [Bha52].

#### (d,n) reactions

The best known direct reactions are stripping reactions, in which, for example, an incident deuteron is stripped of one of its nucleons, which enters the target nucleus, leaving the other to continue an independent life outside (see Fig. 2.2).

The details of such reactions are determined from the properties of the target nucleus, which fixes the energy and the angular momentum with which the proton must enter it. The reaction is not usually observed unless these quantities are correct for forming a well-defined state in the final nucleus.

The orbital angular momentum, $l$, that the proton needs to take it into the target nucleus is determined by the angular momenta and parities of the initial and final nuclear states. Conservation of angular momentum limits $l$ to one of two

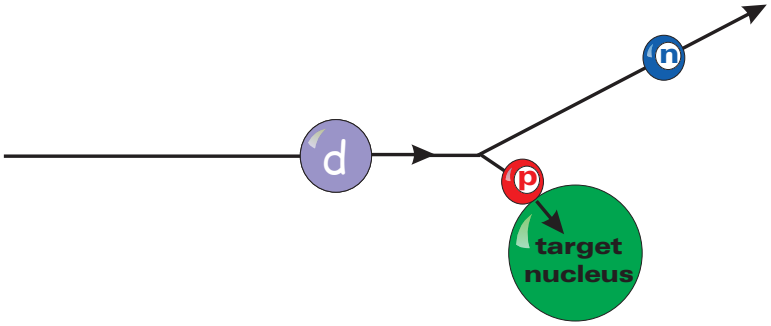


Figure 2.2: A schematic representation of a $(d, n)$ stripping reaction.

consecutive integer values, since the difference between the total angular momenta of the initial and final states must be equal to $l + 1/2$ or $l - 1/2$ (according to whether the proton has its spin parallel or antiparallel to $l$). The conservation of parity (see [Hug71, Per71]) fixes which of the two $l$-values will be effective. If the parities of the initial and final states are the same, $l$ must be even and if the parities of the states are different $l$ must be odd.

The kinetic energy of the neutron is determined by how much of the incident energy of the deuteron is taken into the target nucleus by the proton. In fact it serves to identify the final state produced, by the $Q$-value of the reaction as a whole.

The basic theory of stripping reactions, as outlined by Butler and Hittmair [But57] starts with three approximations, namely that the following interactions may be neglected:

- interaction of the continuing particle (the neutron in a (d,n) reaction and the proton in (d,p) reactions) with the initial nucleus;
- interaction of the neutron with the proton after one of them has entered the target nucleus;
- interaction of the target nucleus with the deuteron as a whole, leading to elastic scattering.

Under these approximations, which are valid for incident deuteron energies

greater than a few million electronvolts, the problem can be written down as an initial wave function describing the target nucleus interacting with an incident plane wave of deuterons, including the internal wave function of the deuteron, and a final wave function obtained. The latter must describe the captured proton inside the nucleus as well as the neutron departing in partial waves, with $l$ determined by the angular momentum with which the proton entered the nucleus. Capture of the protons with a given $l$ thus causes the neutron to depart in a definite set of partial waves, and hence with a characteristic angular distribution. For example, capture with $l = 1$ in the reaction $^{11}$B(d,n)$^{12}$C at 8 MeV gives a first peak in the angular distribution of neutrons at about 20°.

### (d,p) reactions

If it is the neutron that is captured, while the proton remains outside the nucleus, the process is a $(d, p)$ reaction which may be described by a theory differing only marginally from that outlined above. The main difference is that allowance must be made for the Coulomb interaction of the departing particle and the final nucleus. It results in no qualitative changes, but the peaks in the angular distributions are shifted outwards to slightly greater angles. On the other hand, treatment of (d,p) reactions is simpler in that the interaction of the captured particle with the target nucleus contains no Coulomb component.

### Pick-up reactions

With incident energies less than about 5 MeV (n,d) and (p,d) reactions are likely to proceed mainly through compound nucleus formation. At higher energies the inverse of a stripping reaction (a pick-up reaction) may be important. If the target nucleus has an appreciable probability of being found in a state equivalent to a free neutron and a residual nucleus in a state which could exist alone, a passing proton may pick-up the neutron and form a deuteron. For this to happen, the neutron must be in a state which allows it, when free, to have a momentum close

to that of the incident proton; if there is too much discrepancy, the interaction will be too weak to form the deuteron.

## 2.2 Gamma-ray detectors and charged-particle detectors

The study of clustering in nuclei has been carried out over several decades using transfer reactions combined with particle spectroscopy. Studying these nuclei with $\gamma$-ray spectroscopy is of interest because in this case the rotational structure of deformed states can be distinguished through the properties of the $\gamma$-decay. Since the states of interest are populated with very low probabilities, special techniques are required. During the last decade the development of new arrays of germanium detectors with large efficiencies has opened up many new possibilities to study nuclear states populated with very small cross-sections with respect to the total reaction cross section.

### 2.2.1 GASP (GAmma-ray SPectrometer)

The GASP array [Baz92] at the Laboratori Nazionali di Legnaro, Italy, consists of 40 Compton-suppressed, hyper-pure, high-efficiency, n-type germanium detectors (HpGe) which are placed 27 cm from the target (see Fig. 2.3) and cover a total solid angle of 10% of $4\pi$. This corresponds to a total absolute photo-peak efficiency of $\approx$3% at a $\gamma$-ray energy of 1332 keV. These detector systems have been designed to observe, with high efficiency, $\gamma$-ray cascades with high multiplicities from compound reactions, following the evaporation of a few particles (n, p and $\alpha$).

The high selectivity of large arrays of high-purity germanium detectors like GASP is not sufficient by itself to select weakly populated light deformed nuclei. Higher selectivity can be obtained by combining the germanium array with an-

other special ancillary detector which allows triggering on the particle emission of interest. Such a detector is the silicon-ball, which has been developed for the in-beam study of nuclei requiring a high degree of channel selectivity.

Figure 2.3: A picture of the $\gamma$-ray detector array GASP. The second half is moved away. In the centre is the silicon detector ball ISIS.

### 2.2.2 ISIS (Italian SIlicon Sphere)

The ISIS (see Fig. 2.4) consists of 40 silicon $\Delta$E-E telescopes positioned in a compact (16 cm diameter) sphere. Each telescope is composed of two silicon detectors: a thin (130 $\mu$m) detector facing the target, behind which a second thick (1 mm) detector is placed. The ISIS array was developed to serve as an ancillary device for the GASP $\gamma$-ray spectrometer [Far97] and its geometry closely resembles that of GASP, with one telescope in front of every germanium detector. This geometrical configuration has been chosen to minimise the $\gamma$-ray absorption and scattering which would reduce the detection efficiency and the peak-to-total

ratio.

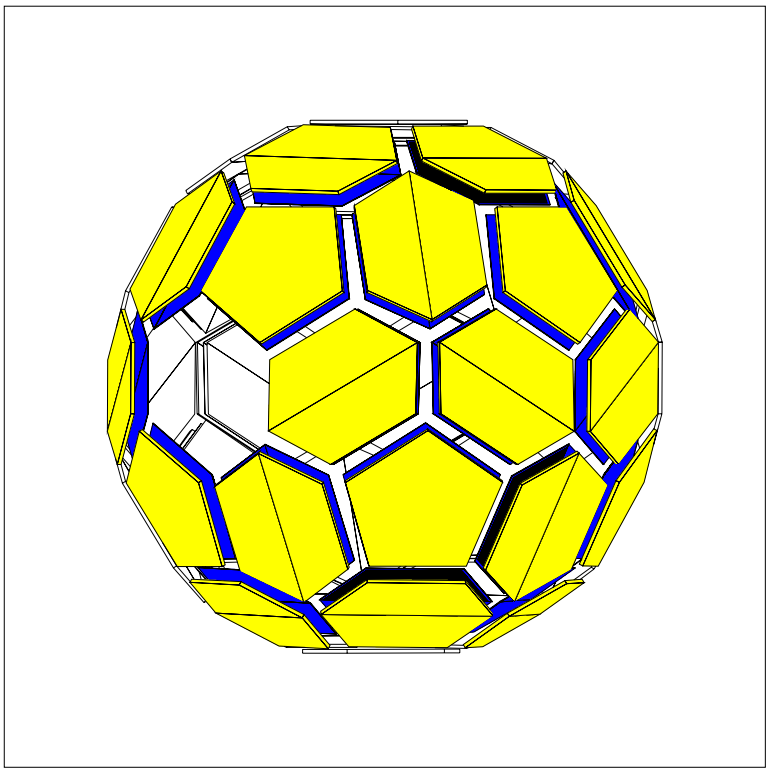

Figure 2.4: Layout of the charged particle detector array ISIS consisting of 40 ΔE-E telescopes.

The energy loss of charged particles in matter can be described using the simplified Bethe-Bloch equation [Kno99]:

$$\frac{dE}{dx} \propto \frac{mZ^2}{E}, \tag{2.2}$$

where $m$ and $Z$ refer to the mass and atomic number of the incoming particle respectively. Plotting the energy signal of the first (thin) detector versus the signal of the second (thick) detector, the events for each different value of the parameter $mZ^2$ will be separated into a distinct 'banana' shaped region. This allows a clean selection to be made on different types of emitted particles.

## 2.3 Data analysis

### 2.3.1 Structure of the data and channel selection

Data are written to magnetic tapes in list mode, which means that every time a new event occurs, the signals from each detector that fires are digitised and written out, together with a number identifying the detector. For the data discussed here, the master trigger is chosen to be GASP and the occurrence of a new event was determined by the condition that at least two Ge-detectors fired in coincidence, within a fixed time window (≈180 ns).

The tapes were read using the GSORT program [Baz97]. This is a general purpose sorting program, which accepts the pre-defined commands written in a common file and user-written subroutines can be implemented. Using this program, raw data can be rearranged in one-, two- and three-dimensional histograms called spectra, matrices and cubes respectively. In the subsequent analysis the histograms were handled using the TRACKN [Baz97] and CMAT [Baz97] programs of the GASP data analysis package.

Since the cross section for the nuclei of interest are smaller than those of many other competing reaction channels it is difficult or even impossible to study their structure using only $\gamma$-ray detectors.

### 2.3.2 Calibrations

When using an array of germanium detectors it is important to have the possibility of summing the data from different detectors. An absolute energy calibration is needed for all individual detectors to deduce the energies of the newly observed $\gamma$-ray transitions. For this reason, data with standard radioactive sources of $^{152}$Eu and $^{56}$Co were collected. Energy calibration coefficients were obtained by fitting the source spectra to produce aligned one dimensional spectra (without further conditions), called projections, for each detector and for each data file.

The projections were subsequently analysed to produce the alignment coefficients matching each run to the reference run (the last in-beam data file was chosen as the reference since this was the closest in time to the runs taken with radioactive sources). This minimised the risk of drifts in the electronics between the experiment and the source calibration runs.

In order to further simplify the analysis an alignment was performed for the silicon detectors. In our case they were simply used to identify the incoming particles, without the need for an absolute energy calibration.

Having calibrated and aligned the energy spectra for the germanium and silicon detectors respectively, the data were sorted into matrices and cubes on disk. A matrix here refers to a two-dimensional histogram where each axis corresponds to a defined quantity, such as the signal of a particular class of detectors or a combination of signals. For example, a $\gamma$-$\gamma$ matrix is generated by histogramming the energy signal of any germanium detector on one axis and on the other axis the energy signal of every other germanium detector that fired in coincidence with the first. Various matrices and cubes were produced with different conditions on the $\gamma$-ray energies and time and on the particle multiplicity.

One has to take into account that the photopeak efficiency of a detector varies with the photon energy, consequently the area of the photopeak in the spectrum will depend both on the absolute number of emitted photons and on the photopeak efficiency at a given energy. One problem encountered when determining the correct intensities of weak transitions is that they are not directly visible in the projection of a matrix. They can only be seen by gating on another transition. Therefore, in order to deduce their intensities, it is necessary to correct for the efficiency at the gating energy.

The relative detector efficiency calibration is determined by analysing the spectra taken with standard radioactive sources of $^{152}$Eu and $^{56}$Co, for which the intensity ratios of the transitions are well known [htt02]. The two sources used here cover the energy range between 40 keV and 3500 keV: at low energies points

on the efficiency curve were provided by the X-rays and $\gamma$-rays coming from the $^{152}$Eu source, the high energy points were obtained from the $^{56}$Co source lines.

To obtain an efficiency calibration for any array of germanium detectors with a similar efficiency response, the spectra of all the Ge-detectors are summed. The resulting spectrum is analysed to find the area of the known peaks, which can be considered as discrete efficiency points. These discrete points can be subsequently fitted with a semi-empirical expression (see Fig. 2.5).

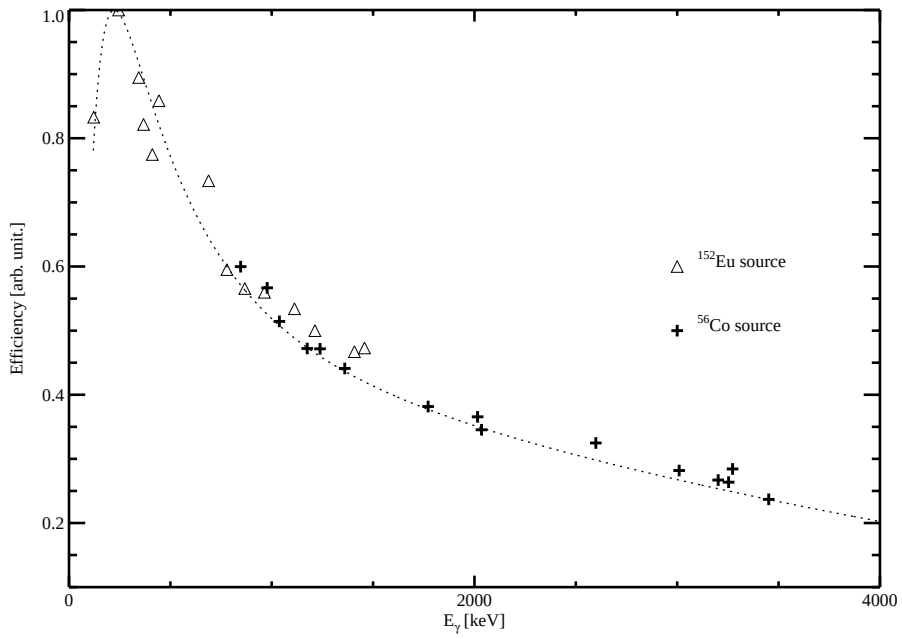


Figure 2.5: Efficiency curve for the Ge-detectors obtained with the standard radioactive sources $^{152}$Eu and $^{56}$Co.

For lines which are out of range of known points on the efficiency curve, an extrapolation using the known efficiency function must be performed, leading to a larger uncertainty in the final transition intensities. For example, for energies higher than 4000 keV (see Fig. 2.5) one should keep in mind the uncertainty arising from the extrapolation.

### 2.3.3 Kinematical corrections and Doppler broadening

The intrinsic resolution of a HPGe crystal is approximately 2-2.5 keV for 1332 keV $\gamma$-rays. The performance of $\gamma$-ray spectrometers is often limited by the Doppler broadening of the lines due to the fact that photons are emitted while the recoiling nucleus is in-flight. The well known expression for the Doppler shift gives the observed energy $E_\gamma$:

$$E_\gamma = E_\gamma^0 \frac{\sqrt{1-\beta}}{1-\beta cos\theta} \approx E_\gamma^0(1+\beta cos\theta), \tag{2.3}$$

where $E_\gamma^0$ is the energy of the emitted $\gamma$-ray if the nucleus is stopped, $\beta$ is the recoil speed, expressed as a fraction of the speed of light and $\theta$ is the angle between the recoil velocity and the direction of observation for the $\gamma$ ray. Differentiating Equation 2.3, yields the broadening of the lines, to first order, induced by the recoil of the residual nuclei:

$$\left|\frac{\Delta E_\gamma^0}{E_\gamma^0}\right|^2 = cos^2\theta \cdot (\Delta\beta)^2 + (\beta sin\theta)^2 \cdot (\Delta\theta)^2 \tag{2.4}$$

Thus, it can be seen that the loss of resolution comes from two components, originating from the dispersion in the recoil velocity and in the angle between the direction of the $\gamma$ ray and the direction of the recoiling compound nucleus. The final effect for typical recoil velocities in fusion-evaporation reactions with $\beta \sim 1 \rightarrow 4\%$ of the velocity of light can easily be of the same order of magnitude (or larger) than the intrinsic resolution of the germanium crystal.

Assuming that the detector covers an infinitesimal solid angle the effect will be that all of the detected photons would be shifted by the same amount with respect to the energies of the emitted photons. Since real detectors cover a finite solid angle, photons will interact within a finite angular range $[\theta - \Delta\theta,\ \theta + \Delta\theta]$ and the effect will be that the peaks will be broadened by a finite amount, which can be estimated to first order as:

$$|\Delta E_\gamma^0| \approx \left| 2\Delta\theta \frac{\partial E_\gamma}{\partial \theta} \right| = 2\Delta E_\gamma^0 \beta |sin\theta| \tag{2.5}$$

where $\Delta\theta$ is half of the opening angle of the detectors. For GASP $\Delta\theta$ is $\approx$14.5° Other effects inducing a velocity dispersion on the recoiling nuclei contribute to the Doppler broadening of the peaks, such as the interaction with the atoms in the target and the evaporation of light particles.

In fusion-evaporation reactions the momentum is conserved, which means that the momentum of the recoiling nucleus, $\vec{p}_R$:

$$\vec{p}_R = \vec{p}_{CN} - \sum_{i=1}^{n} \vec{p}_i \tag{2.6}$$

where $n$ particles are evaporated from the compound nucleus. This implies that,

$$E_\gamma = E_\gamma^0 \left( 1 + \frac{\vec{v}_R}{c} \cdot \vec{d}_\gamma \right) \tag{2.7}$$

where $\vec{d}_\gamma$ is the unit vector in the direction of the emitted $\gamma$-ray. The expression of the observed energy, $E_\gamma$, taking into account the emission of light particles is:

$$E_\gamma = E_\gamma^0 \left( 1 + \frac{m_{CN}}{m_R} \frac{\vec{v}_{CN} \cdot \vec{d}_\gamma}{c} - \sum_{i=1}^{n} \frac{m_i}{m_R} \frac{\vec{v}_i \cdot \vec{d}_\gamma}{c} \right) \tag{2.8}$$

By detecting the emission vector of the evaporated light charged particles it is possible to perform an event by event reconstruction of the velocity of the recoiling nucleus, thus allowing a more precise Doppler shift correction [Sew94]. The effect of this reconstruction is two fold, improving both the effective resolution of the detectors and the peak-to-total ratio. This is equivalent to an increase in the resolving power of the $\gamma$-ray spectrometer, which when combined with the selectivity offered by the coincidences with charged particles, enables the study of nuclei populated with small cross sections.

From the experimental data obtained with ISIS it is not possible to get exact energy measurements for the light charged particles because:

- the energy loss from the particles in the absorbers is *a priori* not known.

• the E-detectors are too thin to stop the high energy protons fully at forward angles.

Therefore, instead of an exact energy a mean value (depending on the angles) is used and optimised with successive approximations. Despite its empirical nature, the method produces good results.